


Ballistic-hydrodynamic phase transition in flow of two-dimensional electrons

A. N. Afanasiev , P. S. Alekseev , A. A. Greshnov, and M. A. Semina
Ioffe Institute, St. Petersburg 194021, Russia

 (Received 7 February 2021; revised 30 September 2021; accepted 5 October 2021; published 11 November 2021)

Phase transitions are characterized by a sharp change in the type of dynamics of microparticles, and their description usually requires quantum mechanics. Recently, a peculiar type of conductor was discovered in which two-dimensional (2D) electrons form a viscous fluid. In this paper we reveal that such an electron fluid in high-quality samples can be formed from ballistic electrons via a phase transition. For this purpose, we theoretically study the evolution of a ballistic flow of 2D weakly interacting electrons with an increase of magnetic field and trace an emergence of a fluid fraction at a certain critical field. Such a restructuring of the flow manifests itself in a kink in the magnetic field dependencies of the longitudinal and the Hall resistances. It is remarkable that the studied phase transition has a classical-mechanical origin and is determined by both the ballistic size effects and electron-electron scattering. Our analysis shows that this effect was apparently observed in recent transport experiments on 2D electrons in graphene and high-mobility GaAs quantum wells.

DOI: [10.1103/PhysRevB.104.195415](https://doi.org/10.1103/PhysRevB.104.195415)

I. INTRODUCTION

Frequent electron-electron collisions in high-quality conductors can lead to the realization of a hydrodynamic regime of charge transport [1]. This regime was recently reported for high-quality graphene [2–6], layered metal PdCoO₂ [7], Weyl semimetals [8], and GaAs quantum wells [9–23]. The formation of the electron fluid was detected by a specific dependence of the resistance on the sample width [7], by the observation of a negative nonlocal resistance [2,3,15,22], giant negative magnetoresistance [8–14,16,17,23], and the magnetic resonance at the double cyclotron frequency [18–21].

Much attention was paid to studies of the transition between the hydrodynamic and nonhydrodynamic regimes of electron transport. In Refs. [5,6] precise measurements of the profiles of the Hall electric field and the current density of two-dimensional (2D) electron flow in graphene stripes were performed. This allowed the authors to detect the Ohmic, the hydrodynamic, and the ballistic flows at varying temperature, electron density, and magnetic field. In particular, a peculiar nonmonotonic magnetoresistance reflecting the ballistic and hydrodynamic transport regimes was observed [5,6]. Similar magnetoresistance was detected in long samples of high-quality GaAs quantum wells [14,16], that, apparently, also evidences the ballistic-hydrodynamic transition. In Refs. [22,23] the transitions from the ballistic to the hydrodynamic regimes in GaAs quantum wells by changing the sample geometry, temperature, and magnetic field were vividly demonstrated.

A theory of 2D electron flow in samples with macroscopic obstacles was constructed in Ref. [24]. In the absence of magnetic field, the ballistic-hydrodynamic transition occurs in such a system by changing the interparticle scattering rate and has a type of a smooth crossover. Another mechanism can be realized for 2D electrons in stripes. A numerical theory of the

ballistic-Ohmic transition and the hydrodynamic transport in long stripes in a perpendicular magnetic field was developed in Ref. [25]. At weak interparticle and disorder scattering rates, the longitudinal and the Hall resistances of a stripe as functions of magnetic field B exhibit kinks at the field $B = B_c$ above which the diameter of the electron cyclotron orbit $2R_c$ becomes smaller than the sample width W . In Ref. [26], for the same system, profiles of the Hall field were calculated. It was shown that an increase of the curvature of the Hall electric field characterizes the transition from the ballistic to the hydrodynamic regimes.

In Refs. [27–29] it was demonstrated that the interparticle scattering induces the corrections to the ballistic conductance of a wide ballistic microcontact between two metal bulk samples. Such corrections should be regarded as precursors of the hydrodynamic regime. In Ref. [30] such positive corrections were observed in a GaAs/AlGaAs based ballistic microcontact. In Refs. [31,32] similar hydrodynamic corrections to the conductance and the Hall field were theoretically studied for a long ballistic sample with rough edges.

Here, we demonstrate that the hydrodynamic regime of transport of 2D electrons in high-quality stripes is formed from the ballistic regime via a genuine phase transition with an increase of magnetic field B . For this purpose, we consider a long stripe with straight but rough edges. First, we reveal that in the lower vicinity of the critical field, $0 < B_c - B \ll B_c$, the momentum relaxation due to collisions of electrons with the stripe edges becomes strongly suppressed due to the ballistic size effects, thus even weak electron-electron scattering begins to be important for the flow formation. Second, we show that in the upper vicinity of B_c , $0 < B - B_c \ll B_c$, the emerging “central” electrons, which are not scattered at the edges, critically change the type of electron distribution and become the nucleus of a collectivized fluid phase. We develop a mean-field model based on the classical kinetic equation

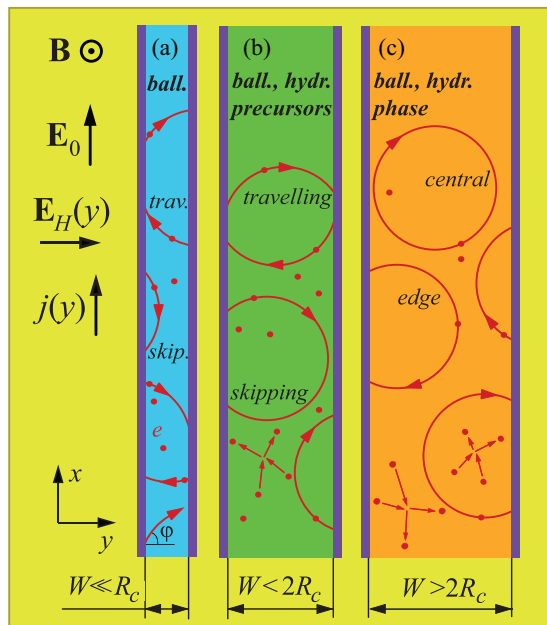


FIG. 1. Two-dimensional electrons in a long sample at (a) low, $W \ll R_c$, (b) intermediate, $W \sim R_c$, $W < 2R_c$, and (c) moderately high, $W \sim R_c$, $W > 2R_c$, magnetic fields. The ballistic-hydrodynamic phase transition occurs at the critical field B_c corresponding to $2R_c = W$. In its lower vicinity, $0 < B_c - B \ll B_c$, electrons moving along the skipping orbits close to complete cyclotron circles undergo slow momentum relaxation. They are precursors of hydrodynamic flow. Above the critical point, $B > B_c$, a group of central electrons appear which do not collide with the edges, representing the nucleus of the hydrodynamic fluid phase.

to describe these critical transport regimes of the ballistic-hydrodynamic phase transition. Our analysis of the results of the experiments [5,6,16] evidences that the formation of a hydrodynamic regime from a ballistic one was realized in them via such a phase transition.

Using the developed approach, we also obtain results on the ballistic transport in stripes at low magnetic fields, $B \ll B_c$. In particular, we show that the interplay of the ballistic effects and the interparticle scattering induces a strongly nonuniform electron flow and a nontrivial character of the Hall effect. A similar anomalously large Hall effect was recently theoretically obtained in Ref. [33] for asymmetric stripes with one rough and the other specular edges.

II. BALLISTIC REGIME

We consider a flow of 2D degenerate electrons in a long sample with rough edges in a perpendicular magnetic field \mathbf{B} (see Fig. 1). Electrons are diffusively scattered on the rough sample edges leading to momentum relaxation. In the bulk of the sample, electrons collide with each other and their total momentum is conserved. We assume that the rate γ of the electron-electron scattering is weak, $W \ll l$, where $l = v_F/\gamma$ is the mean free path and v_F is the Fermi velocity. We describe the transport in this system by the nonequilibrium part $\delta f(y, \varphi, \varepsilon)$ of the distribution function $f = f_F + \delta f$ deter-

mined by the linearized kinetic equation,

$$v_F \cos \varphi \frac{\partial \delta f}{\partial y} + \frac{e}{m} \mathbf{E} \cdot \frac{\partial f_F}{\partial \mathbf{v}} - \omega_c \frac{\partial \delta f}{\partial \varphi} = \text{St}[\delta f], \quad (1)$$

with the diffusive boundary conditions at $y = \pm W/2$. Here, ε is the electron energy, φ is the angle of the electron velocity $\mathbf{v}/v_F = (\cos \varphi, \sin \varphi)$, f_F is the Fermi distribution, $\omega_c = v_F/R_c$ is the cyclotron frequency, e and m are the electron charge and mass, $\mathbf{E} = \mathbf{E}_0 + \mathbf{E}_H$ is the total electric field, \mathbf{E}_0 is the applied field, \mathbf{E}_H is the Hall field, and $\text{St}[\delta f] = -\gamma (\delta f - \hat{P}[\delta f])$ is the simplified interparticle collision operator, in which \hat{P} is the projector onto the zeroth and first harmonics of δf by φ .

At magnetic fields B below the critical field, $B < B_c$, when $2R_c > W$, each electron is predominantly scattered at the edges. The transport is ballistic in almost all such B , and the interparticle collisions can constrain the time which electrons spend on the ballistic trajectories. Our analysis [34] based on Eq. (1) shows that the ballistic regime has a fine structure, namely, it is divided into three subregimes.

In the first ballistic subregime of low fields, $B \ll B_c(W/l)^2$, the electron trajectories are almost straight. Their maximum length is limited by the interparticle scattering length l . This subregime was studied in Refs. [31,32] and in this work [34]. Depending on the arrangement of trajectories, electrons are divided on the two groups: the “traveling electrons” which, after scattering on an edge, reach the other edge or scatter in the bulk, and the “skipping electrons” which return to the same edge after scattering on it [see Figs. 1(a) and 1(b)]. Most electrons belong to the first type. Electrons of the second type are located in the edge vicinities, $W/2 - |y| \lesssim l^2/R_c$, and their velocity angles are $\varphi \approx \pm\pi/2$.

In the central part of the sample, $W/2 - |y| \gg l^2/R_c$, the Hall electric field $E_H(y)$ is related to the dynamics of the “traveling electrons” [34]. The resulting local Hall resistance, $\varrho_{xy}(y) = E_H(y)/j(y)$, turns out to be one half of the Hall resistance of the macroscopic Ohmic samples [32],

$$\varrho_{xy} = \frac{1}{2} R_H^{(0)} B, \quad R_H^{(0)} = \frac{1}{n_0 e c}, \quad (2)$$

where $j(y)$ is the current density, n_0 is the electron density, and c is the velocity of light. In Ref. [32] this result was obtained from a straightforward solution of kinetic equation (1). In this work we reveal [34] the physical essence of result (2). Namely, the value E_H yielding Eq. (2) corresponds to the balance of the Hall force eE_H and the component of the Lorentz force $\Delta F_{L,y}(t) = eBa_x t/c$, averaged over all traveling electrons in the region $W/2 - |y| \gg l^2/R_c$. Here, $a_x = eE_0/m$ is the acceleration of electrons by the field E_0 and $t = t(y, \varphi)$ is the time passed since the scattering at the edge.

In the vicinities of the edges, $W/2 - |y| \lesssim l^2/R_c$, the Hall field $E_H(y)$ and the current density $j(y)$ are strongly affected by the skipping electrons. The profile $E_H(y)$ becomes strongly inhomogeneous [see Fig. 2(b)]. The profile $j(y)$ is approximately homogeneous, but the non-perturbative correction to its mean value is independent on the magnetic field in the central region, $W/2 - |y| \gg l^2/R_c$, and depends on B in the near-edge regions $W/2 - |y| \lesssim l^2/R_c$. The resulting values of $E_H(y)$ and $j(y)$ in the edge vicinities determine the resistances

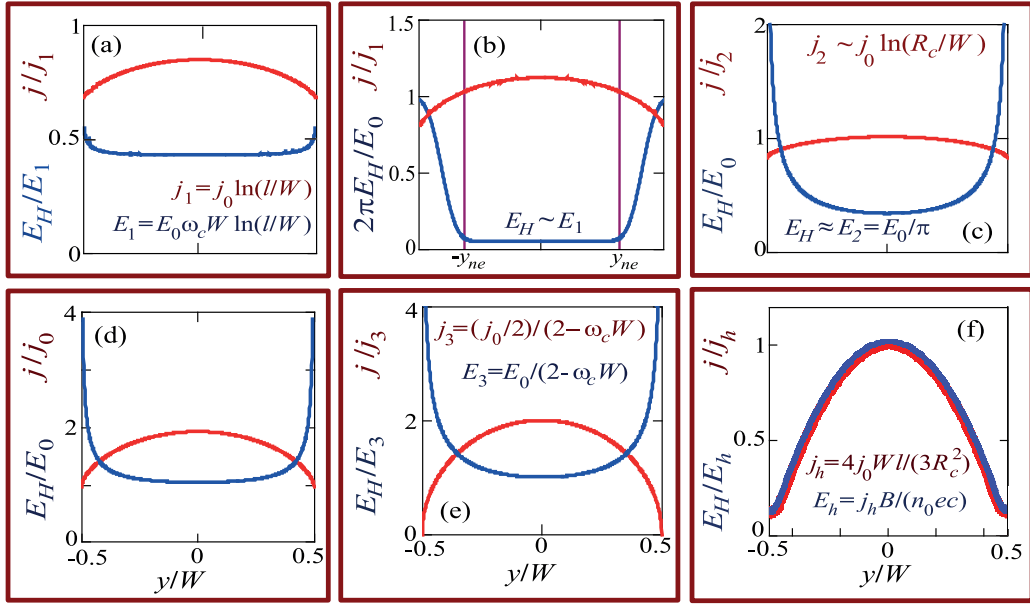


FIG. 2. Current density $j(y)$ and Hall electric field $E_H(y)$ at various magnetic fields B : (a) the first ballistic subregime, in the limit $B \rightarrow 0$ (only the flow in the central part of the sample, $W/2 - |y| \gg l^2/R_c$, is shown); (b) the middle part of the first ballistic subregime, $R_c \gg l^2/W$ [schematically; violet lines depict the boundaries of the near-edge regions where skipping electrons propagate, $y_{ne} \approx \pm(W/2 - l^2/R_c)$]; (c) the second ballistic subregime, $W \ll R_c \ll l^2/W$; (d) the middle part of the third ballistic subregime, $0 < 2R_c/W - 1 \sim 1$; (e) the upper part of the third ballistic subregime near the critical field, $W/l \ll 2R_c/W - 1 \ll 1$; and (f) the hydrodynamic regime with a Poiseuille flow, $W \gg R_c$ (schematically).

ϱ_{xx} and ϱ_{xy} of the whole sample, provided it is sufficiently long and straight [34].

In the second ballistic subregime, $B_c(W/l)^2 \ll B \ll B_c$, electron trajectories become substantially bent. Their maximal length is now limited by their geometry. This subregime was studied in Ref. [25] by a numeric solution of Eq. (1) and in Ref. [26] by its analytical solution accounting only for the departure term $-\gamma \delta f$ in the operator St. The resulting longitudinal and Hall resistances exhibit the singular behavior, $\varrho_{xx,xy}(B) \sim 1/\ln(\sqrt{R_c/W})$, originating from the shortening of the longest ballistic trajectories with an increase of B [34].

In the third ballistic subregime, $B_c W/l \ll B_c - B \lesssim B_c$, the number of skipping electrons becomes relatively large: comparable to or even greater than the number of traveling ones [see Fig. 1(b)]. In order to satisfy the condition $j_y = 0$ of the absence of the transverse current, the $\mathbf{E}_0 \times \mathbf{B}$ drift contribution related to all electrons, $j_y^{(0)} = n_0 e c E_0 / B$, is compensated by the excess and the deficiency of nonequilibrium traveling electrons with $v_y(t) > 0$ and with $v_y(t) < 0$. Nonequilibrium skipping electrons do not compensate $j_y^{(0)}$, as $v_y(t) > 0$ and $v_y(t) < 0$ symmetrically for each skipping trajectory. The diffusive reflection of electrons from the edges occurs with equal probabilities for all φ . Thus, at $2R_c/W - 1 \ll 1$, when the skipping electrons dominate, the whole electron density strongly increases (as compared with the case $2R_c/W - 1 \sim 1$) in order to compensate $j_y^{(0)}$ by the relatively small part of the traveling electrons.

This dynamics is described by the distribution [34]

$$\delta f(y, \varphi, \varepsilon) = \chi(y, \varphi) f'_F(\varepsilon) \frac{E_0}{\omega_c u}, \quad (3)$$

where the behavior of the factor χ , $\chi(y, \varphi) \approx 1$ at $-\pi + \varphi_- < \varphi < \varphi_+$ and $\chi(y, \varphi) \approx -1$ at $\varphi_+ < \varphi < \pi + \varphi_-$, reflects the domination of the skipping electrons (here, $\varphi_{\pm}(y) = \arcsin[1 - (W/2 \pm y)/R_c]$). The small parameter $u(B) = (2/\pi)(2 - W/R_c) \ll 1$ in Eq. (3) shows how close B is to the critical field B_c . The resulting current density and the Hall field in the main order by u take the form

$$j(y) = \frac{2r(y)j_0}{\pi u}, \quad E_H(y) = \frac{2E_0}{\pi r(y)u}, \quad (4)$$

where $j_0 = n_0 e^2 E_0 W / (v_F m)$ and $r(y) = \sqrt{1 - (y/R_c)^2}$. The magnitudes of $j(y)$ and $E_H(y)$ rapidly increase as B approaches B_c due to the factor u in the denominators of Eqs. (4). The averaged resistances $\varrho_{xx} = E_0 / \langle j(y) \rangle$ and $\varrho_{xy} = \langle E_H(y) \rangle / \langle j(y) \rangle$ [the angle brackets $\langle \cdot \rangle$ denote averaging by y] corresponding to distribution (3) in the two main orders by the small parameter \sqrt{u} take the form

$$\varrho_{xx}(B) = 2\varrho_0 u, \quad \varrho_{xy}(B) = R_H^{(0)} B F(u), \quad (5)$$

where $\varrho_0 = E_0 / j_0$ and $F(u) = 1 - \sqrt{u/\pi}$. The vanishing of ϱ_{xx} as $\sim u$ reflects the transitional character of the ballistic electron dynamics at $B \rightarrow B_c$ [see Fig. 1(b)].

The evolution of $j(y)$ and $E_H(y)$ in the ballistic subregimes with an increase of B are shown in Figs. 2(a)–2(e).

III. PHASE TRANSITION

At the fields B in the upper and the lower vicinities of B_c , $|B - B_c| \ll B_c$, most of the electrons are the “edge electrons” that move along the skipping trajectories hitting one of the edges. In the upper vicinity, when $W > 2R_c$, a small

group of “central electrons” arise which never touch the edges [Fig. 1(c)].

In the nearest lower vicinity of B_c , $0 < B_c - B \lesssim B_c W/l$, the imbalance densities of the left-edge and the right-edge skipping electrons increase dramatically, as the ballistic distribution function (3) and values (4) diverge by $u \rightarrow 0$ at $W/l \rightarrow 0$. Therefore the electron dynamics at such B is to be controlled not only by their scattering on the edges, but also by interparticle collisions.

To describe such semiballistic flow, first we calculate [34] the trial distribution function, similar to the purely ballistic function (3), but additionally accounting for the departure term $-\gamma \delta f$ in the operator St in Eq. (1):

$$\delta f_d(y, \varphi, \varepsilon) = \chi(y, \varphi) f'_F(\varepsilon) \frac{E_0/\omega_c}{u + W/l}. \quad (6)$$

The averaged current density and the Hall field corresponding to δf_d rapidly increase at $B \rightarrow B_c$ up to values limited by the slow scattering rate $\gamma = v_F/l$:

$$j_d = \frac{j_0/2}{u + W/l}, \quad E_{H,d} = \frac{E_0 F(u)}{u + W/l}. \quad (7)$$

Second, to describe the flow at $0 < B_c - B \lesssim B_c W/l$, we need to account for the effect of the arrival term $\gamma \hat{P}[\delta f]$ in Eq. (1). Indeed, the departure term $-\gamma \delta f$ dominates in the first ballistic subregime [31], and both the departure and the arrival terms are relatively small in the second and third ballistic subregimes [26,34], whereas in a well-formed hydrodynamic flow at $W \gg R_c$ they are close to one another [31]. An estimate shows that for function f_d (6) at $0 < 2R_c - W \lesssim W^2/l$ these two terms have values of the same order of magnitude. In this connection, we propose a mean-field model based on the approximation of the arrival term $\gamma \hat{P}[\delta f]$ [34] by its averaged by y value, whose main part is $\gamma \sin \varphi j/(n_0/m)$ (here j is the actual averaged current density). After this substitution, the external field E_0 in kinetic equation (1) is changed on the effective one:

$$E_0 \rightarrow \tilde{E}_0 = E_0 + \gamma \frac{j}{n_0/m}. \quad (8)$$

As a result, the self-consistent distribution f and averaged current density j are given by semiballistic formulas (6) and (7) with $E_0 \rightarrow \tilde{E}_0$. For j we obtain

$$j = \frac{1}{2} \frac{j_0 + j W/l}{u + W/l}. \quad (9)$$

This mean-field-type equation accounts for the redistribution of momentum between the skipping electrons in their collisions with each other, while formulas (6) and (7) imply the relaxation of momentum in the scattering of electrons in the bulk. The solution of Eq. (9) is $j = j_0/[2u + W/l]$. To find the Hall field near the critical point, we should substitute the renormalization $E_0 \rightarrow \tilde{E}_0$ in the semiballistic value $E_{H,d}$ (7), which yields $E_H = E_0 F(u)/[u + W/(2l)]$.

In the upper vicinity of the transition point, $0 < B - B_c \ll B_c$, when the relative density of the central electrons is small, $\alpha_c = (W - 2R_c)/W \ll 1$, each edge electron is still scattered predominantly on the edges and on the other edge electrons. Similarly as for the flow in the lower vicinity of B_c , $0 < B_c - B \ll B_c$, the distribution function of these electrons δf_e is given by a formula based on the semiballistic distribution

δf_d (6). Therefore the departure and the arrival terms of St in Eq. (1) with this δf_e are also of the same order of magnitude. To account for the arrival term $\gamma P[\delta f]$, we again substitute it by its averaged value, which is mainly proportional to the averaged current $j = j_e + j_c$ corresponding to $\delta f = \delta f_e + \delta f_c$. As a result, the function δf_e is given by Eq. (6) at $u = 0$ with the sample width W changed on the width $\tilde{W} = 2R_c$ of the subregion with the edge electrons and the renormalized electric field:

$$E_0 \rightarrow \tilde{E}_0 = E_0 + \gamma \frac{j_e + j_c}{n_0/m}. \quad (10)$$

Correspondingly, an analysis shows that for the current component j_e we should use Eq. (9) at $u = 0$ with $j = j_e + j_c$ and the density factor $\alpha_e = \tilde{W}/W$.

All the central electrons have almost coinciding trajectories and are scattered mainly by the edge ones [see Fig. 1(c)]. Thus the flow of the central electrons is similar to an Ohmic one, and their component j_c is given by the Drude formula with the density factor α_c and the same \tilde{E}_0 . In the distribution of the central electron δf_c the first angular harmonic dominates, unlike the semiballistic function δf_b (6), which is discontinuous in φ and thus contains many comparable harmonics by φ [34].

We arrive at the mean-field equations for j_e and j_c [34],

$$\begin{aligned} j_e &= (\alpha_e/2)(j_{cr} + j_e + j_c), \\ j_c &= \alpha_c(j_{cr} + j_e + j_c), \end{aligned} \quad (11)$$

where $j_{cr} = j_0 l/W = n_0 e^2 E_0 l/(v_F m)$. These equations are similar in their meaning to the one-component equation (9), but account for the appearance at $B > B_c$ of the two electron species. The solution of (11) yields $j = (1 + 2\alpha_c)j_{tr}$.

The Hall field is also related to the edge and central electrons: $E_H = E_{H,e} + E_{H,c}$. The first term is calculated by Eq. (7) at $u = 0$ with the factor α_e and the substitutions $E_0 \rightarrow \tilde{E}_0$ and $W \rightarrow \tilde{W}$. According to the Ohmic-like form of the distribution δf_c , the term $E_{H,c}$ is given by the Drude formula $E_{H,c} = \omega_c j_c/(n_0/m)$. As a result, we obtain $E_H = (1 + 2\alpha_c)(l/R_c)E_0$.

The described change in electron dynamics above and below the critical field is reflected in the kinks in the obtained magnetic dependencies $j(B)$ and $E_H(B)$. Next, for q_{xx} in the main orders by $|b| \ll 1$ and $W/l \ll 1$ we obtain [34]

$$\frac{q_{xx}(B)}{q_{cr}} = 1 - b \times \begin{cases} 8l/(\pi W), & b < 0, |b| \ll 1, \\ 2, & 0 < b \ll 1, \end{cases} \quad (12)$$

where $q_{cr} = E_0/j_{cr}$ and $b = (B - B_c)/B_c$. For the Hall resistance $q_{xy}(B)$ in the main order by W/l and the two first orders by $\sqrt{|b|}$ we obtain the same result as in Eqs. (5) at $b < 0$, while at $b > 0$ the above formulas for j and E_H yield $q_{xy}(B) \equiv R_H^{(0)} B$. The kinks in the obtained longitudinal and Hall resistances at $B = B_c$ evidence that the formation of the hydrodynamic flow from the ballistic one is realized via a phase transition.

Note that the derivative $\partial q_{xx}/\partial B$ is proportional to γ in the hydrodynamic vicinity of the critical point, $B > B_c$, and is independent on γ in the ballistic vicinity, $B < B_c$. This indicates the critically larger role of the interparticle collisions in the hydrodynamic phase than their role in the ballistic phase.

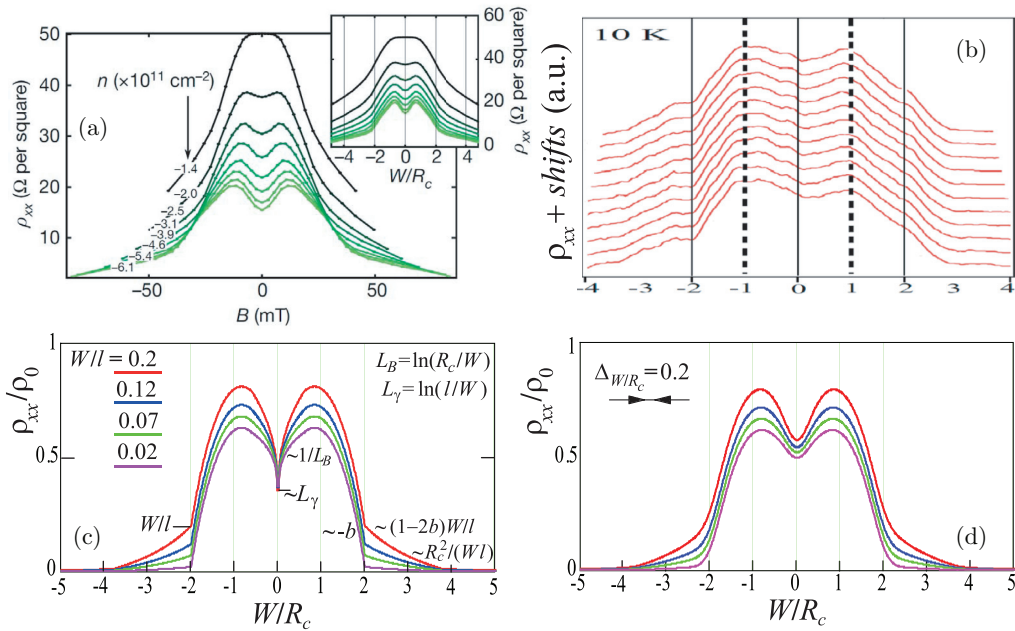


FIG. 3. Longitudinal resistance ρ_{xx} of long samples as a function of magnetic field $B \propto W/R_c$. (a) and (b) present experimental results for graphene stripes and are taken from Refs. [5,6], respectively. Different curves correspond to varying 2D electron densities, controlled by the gate voltages. Distortions of the curves in (b), asymmetric in B , can be due to some contribution from the Hall resistance ρ_{xy} in the measured data. (c) Results of our theory for several interparticle scattering rates γ . In (d) we plot the curves from (c), smoothed by convolution with a Gaussian weight function $G_{\Delta}(B)$ with the width Δ_{W/R_c} , that simulates the contribution from sample corners, several sections of a long sample with varying widths, and other imperfections.

With the increase of B and α_c , the collisions between the central electrons become important, therefore j_c becomes nonuniform by y . The hydrodynamic-ballistic flow at $\alpha_c \sim 1$ was numerically studied in Refs. [25,26]. At $\alpha_c \gg 1$ the central electrons dominate everywhere except the edge vicinities, $W/2 - |y| \sim R_c$, and the Poiseuille flow $j_c(y) \sim (W/2)^2 - y^2$ is formed [see Fig. 2(f)]. The resulting resistance ρ_{xx} is determined by the viscosity $\rho_{xx} \sim \eta_{xx}/W^2$, $\eta_{xx} \sim \gamma/\omega_c^2$, while the Hall resistance ρ_{xy} is close to $\rho_{xy}^{(0)} = R_H^{(0)}B$ [17].

In Fig. 3 we compare the results of experiments [5,6] on 2D electron transport in high-quality graphene stripes with our theoretical results. Both theoretical and experimental resistances ρ_{xx} have similar profiles, including the minimum at $W/R_c \ll 1$, the maximum at $W/R_c \sim 1$, and the kink at $W/R_c = 2$. Convolution of the calculated dependencies $\rho_{xx}(B)$ with a weight function $G_{\Delta}(B)$, simulating the imperfection of the sample, leads to a very good agreement of the shapes of the observed and calculated curves [compare Figs. 3(a) and 3(d)]. In the Supplemental Material [34] we also compare our results with preceding theories [25,26] and other related experiments [9–11,16]. The numerical solution [25] of Eq. (1) for the stripes in which the scattering on disorder dominates leads to the dependencies $\rho_{xx,xy}(B)$ almost identical to the ones calculated within our theory based on Eq. (1) with the inter-particle collision operator replaced by the operator describing the electron scattering on disorder $\text{St} = \text{St}_{\text{dis}}$ (see details in the Supplemental Material [34]). Our results for the second ballistic subregime coincide with the ones obtained in Ref. [26]. The longitudinal and Hall resistances observed in

Ref. [16] in long samples of GaAs quantum wells are in a good agreement with the calculated dependencies $\rho_{xx,xy}(B)$ [34].

IV. CONCLUSION

The phase transition between the ballistic and the hydrodynamic transport with the increase of a magnetic field regimes has been revealed and theoretically studied for weakly interacting 2D electrons in long pure samples. An analysis of magnetotransport experiments [5,6,16] on high-quality stripes of graphene and a GaAs quantum well shows that this transition was apparently observed in them.

We think that the phase transitions of the types considered here can be possible in a wide class of high-purity 2D and 3D materials for the samples in which defectless regions are confined by edges of different shapes. These phase transitions can differ by types of electron energy spectra, character of the electron-electron scattering, and shapes of the samples. For example, samples with ballistic microcontacts studied in Refs. [27–30] may be of great interest. The phase transitions of such a type are to be characterized by (i) a kink in the dependence of the Hall and the longitudinal sample resistances on magnetic field and (ii) a change of the type of temperature dependences of the derivative of the longitudinal resistance by magnetic field. Therefore they may be considered as a classical-mechanics analog of the metal-insulator transition in doped semiconductors as well as of the normal metal-superconductor phase transition.

ACKNOWLEDGMENTS

We thank Yu. O. Alekseev, A. I. Chugunov, A. P. Dmitriev, L. E. Golub, V. S. Khrapai, A. A. Shevyrin, and A. V. Shumilin for many fruitful discussions. The study was supported by

the Russian Foundation for Basic Research (Grant No. 19-02-00999) and by the Foundation for the Advancement of Theoretical Physics and Mathematics “BASIS.”

-
- [1] R. N. Gurzhi, *Sov. Phys. Usp.* **94**, 657 (1968).
- [2] D. A. Bandurin, I. Torre, R. Krishna Kumar, M. Ben Shalom, A. Tomadin, A. Principi, G. H. Auton, E. Khestanova, K. S. Novoselov, I. V. Grigorieva, L. A. Ponomarenko, A. K. Geim, and M. Polini, *Science* **351**, 1055 (2016).
- [3] L. Levitov and G. Falkovich, *Nat. Phys.* **12**, 672 (2016).
- [4] A. I. Berdyugin, S. G. Xu, F. M. D. Pellegrino, R. Krishna Kumar, A. Principi, I. Torre, M. Ben Shalom, T. Taniguchi, K. Watanabe, I. V. Grigorieva, M. Polini, A. K. Geim, and D. A. Bandurin, *Science* **364**, 162 (2019).
- [5] J. A. Sulpizio, L. Ella, A. Rozen, J. Birkbeck, D. J. Perello, D. Dutta, M. Ben-Shalom, T. Taniguchi, K. Watanabe, T. Holder, R. Queiroz, A. Principi, A. Stern, T. Scaffidi, A. K. Geim, and S. Ilani, *Nature (London)* **576**, 75 (2019).
- [6] M. J. H. Ku, T. X. Zhou, Q. Li, Y. J. Shin, J. K. Shi, C. Burch, L. E. Anderson, A. T. Pierce, Y. Xie, A. Hamo, U. Vool, H. Zhang, F. Casola, T. Taniguchi, K. Watanabe, M. M. Fogler, P. Kim, A. Yacoby, and R. L. Walsworth, *Nature (London)* **583**, 537 (2020).
- [7] P. J. W. Moll, P. Kushwaha, N. Nandi, B. Schmidt, and A. P. Mackenzie, *Science* **351**, 1061 (2016).
- [8] J. Gooth, F. Menges, C. Shekhar, V. Suess, N. Kumar, Y. Sun, U. Drechsler, R. Zierold, C. Felser, and B. Gotsmann, *Nat. Commun.* **9**, 4093 (2018).
- [9] L. Bockhorn, P. Barthold, D. Schuh, W. Wegscheider, and R. J. Haug, *Phys. Rev. B* **83**, 113301 (2011).
- [10] A. T. Hatke, M. A. Zudov, J. L. Reno, L. N. Pfeiffer, and K. W. West, *Phys. Rev. B* **85**, 081304(R) (2012).
- [11] R. G. Mani, A. Kriisa, and W. Wegscheider, *Sci. Rep.* **3**, 2747 (2013).
- [12] Q. Shi, P. D. Martin, Q. A. Ebner, M. A. Zudov, L. N. Pfeiffer, and K. W. West, *Phys. Rev. B* **89**, 201301(R) (2014).
- [13] L. Bockhorn, I. V. Gornyi, D. Schuh, C. Reichl, W. Wegscheider, and R. J. Haug, *Phys. Rev. B* **90**, 165434 (2014).
- [14] G. M. Gusev, A. D. Levin, E. V. Levinson, and A. K. Bakarov, *AIP Adv.* **8**, 025318 (2018).
- [15] A. D. Levin, G. M. Gusev, E. V. Levinson, Z. D. Kvon, and A. K. Bakarov, *Phys. Rev. B* **97**, 245308 (2018).
- [16] G. M. Gusev, A. D. Levin, E. V. Levinson, and A. K. Bakarov, *Phys. Rev. B* **98**, 161303(R) (2018).
- [17] P. S. Alekseev, *Phys. Rev. Lett.* **117**, 166601 (2016).
- [18] Y. Dai, R. R. Du, L. N. Pfeiffer, and K. W. West, *Phys. Rev. Lett.* **105**, 246802 (2010).
- [19] A. T. Hatke, M. A. Zudov, L. N. Pfeiffer, and K. W. West, *Phys. Rev. B* **83**, 121301(R) (2011).
- [20] M. Bialek, J. Lusakowski, M. Czapkiewicz, J. Wrobel, and V. Umansky, *Phys. Rev. B* **91**, 045437 (2015).
- [21] P. S. Alekseev and A. P. Alekseeva, *Phys. Rev. Lett.* **123**, 236801 (2019).
- [22] A. C. Keser, D. Q. Wang, O. Klochan, D. Y. H. Ho, O. A. Tkachenko, V. A. Tkachenko, D. Culcer, S. Adam, I. Farrer, D. A. Ritchie, O. P. Sushkov, and A. R. Hamilton, *Phys. Rev. X* **11**, 031030 (2021).
- [23] A. Gupta, J. J. Heremans, G. Kataria, M. Chandra, S. Fallahi, G. C. Gardner, and M. J. Manfra, *Phys. Rev. Lett.* **126**, 076803 (2021).
- [24] H. Guo, E. Ilseven, G. Falkovich, and L. Levitov, *Proc. Natl. Acad. Sci. USA* **114**, 3068 (2017).
- [25] T. Scaffidi, N. Nandi, B. Schmidt, A. P. Mackenzie, and J. E. Moore, *Phys. Rev. Lett.* **118**, 226601 (2017).
- [26] T. Holder, R. Queiroz, T. Scaffidi, N. Silberstein, A. Rozen, J. A. Sulpizio, L. Ella, S. Ilani, and A. Stern, *Phys. Rev. B* **100**, 245305 (2019).
- [27] K. E. Nagaev and O. S. Ayvazyan, *Phys. Rev. Lett.* **101**, 216807 (2008).
- [28] K. E. Nagaev and T. V. Kostyuchenko, *Phys. Rev. B* **81**, 125316 (2010).
- [29] K. E. Nagaev, *Phys. Rev. B* **102**, 045426 (2020).
- [30] M. Yu. Melnikov, J. P. Kotthaus, V. Pellegrini, L. Sorba, G. Biasiol, and V. S. Khrapai, *Phys. Rev. B* **86**, 075425 (2012).
- [31] P. S. Alekseev and M. A. Semina, *Phys. Rev. B* **98**, 165412 (2018).
- [32] P. S. Alekseev and M. A. Semina, *Phys. Rev. B* **100**, 125419 (2019).
- [33] Yu. O. Alekseev and A. P. Dmitriev, *Phys. Rev. B* **104**, 085434 (2021).
- [34] See Supplemental Material at <http://link.aps.org/supplemental/10.1103/PhysRevB.104.195415> for the details of the theory and of the comparison of its results with preceding works, which contains Refs. [35–45].
- [35] C. Beenakker and H. van Houten, in *Semiconductor Heterostructures and Nanostructures*, edited by H. Ehrenreich and D. Turnbull, Solid State Physics (Academic, New York, 1991), Vol. 44, pp. 1–228.
- [36] P. S. Alekseev and A. P. Dmitriev, *Phys. Rev. B* **102**, 241409(R) (2020).
- [37] T. J. Thornton, M. L. Roukes, A. Scherer, and B. P. Van de Gaag, *Phys. Rev. Lett.* **63**, 2128 (1989).
- [38] D. K. C. MacDonald, *Nature (London)* **163**, 639 (1949).
- [39] E. H. Sondheimer, *Phys. Rev.* **80**, 401 (1950).
- [40] D. K. C. MacDonald and R. Sarginson, *Proc. R. Soc. London, Ser. A* **759**, 223 (1950).
- [41] E. Ditlefsen and J. Lothe, *Philos. Mag.* **14**, 759 (1966).
- [42] E. M. Baskin, L. N. Magarill, and M. V. Entin, *Sov. Phys. JETP* **48**, 365 (1978).
- [43] A. V. Bobylev, F. A. Maa, A. Hansen, and E. H. Hauge, *Phys. Rev. Lett.* **75**, 197 (1995).
- [44] A. Dmitriev, M. Dyakonov, and R. Jullien, *Phys. Rev. B* **64**, 233321 (2001).
- [45] Y. M. Beltukov and M. I. Dyakonov, *Phys. Rev. Lett.* **116**, 176801 (2016).